A Novel Intuitionistic Fuzzy Set Approach for Segmentation of Kidney MR Images

Shreyas Mushrif[1], Aldo Morales[1], Christopher Sica[2], Qing.X Yang[2], Susan Eskin[1], Lawrence Sinoway[3]

[1]Department of Electrical Engineering, Pennsylvania State University, Harrisburg, Middletown PA , US
[2]Department of Radiology, Pennsylvania State University, College of Medicine, Hershey PA, US
[3]Heart and Vascular Institute, Pennsylvania State University, College of Medicine, Hershey PA, US

Abstract— **This paper presents a novel algorithm, which uses intuitionistic fuzzy sets and rough set theory to segment the renal components in kidney MR images. A new membership function is proposed and then is used to obtain an intuitionistic fuzzy model of the image to compensate the inherent heterogeneity present among the different renal tissue classes. In addition, a new method, which uses Hamming distance is proposed to calculate the histon. The histon is then used to compute intuitionistic fuzzy roughness measure which yields optimum valley points for image segmentation. The proposed algorithm segments the kidney MR images into medulla, cortex, and blood vessels. The quantitative performance evaluation indicates better performance of the proposed algorithm over a competing technique.**

Keywords—Hamming distance, kidney MR image, intuitionistic fuzzy set, histon, restricted equivalence function, segmentation.

I. INTRODUCTION

Magnetic resonance imaging (MRI) is a non-invasive and safe modality, and has recently emerged as an effective research tool to study human kidney function. Kidney MR images provide excellent soft tissue contrast which enables differentiation between medulla and cortex. In addition, an emerging area has been the use of blood oxygenation level dependent (BOLD) MRI to study kidney function. These functional studies require accurate segmentation of the kidney into medulla, cortex, arterial, and pelvic compartments However, the task of segmentation is very challenging due to thermal noise in the body, intensity inhomogeneity due to RF coil shading, inherent heterogeneity present among the tissue classes, patient motion, and partial volume effects due to inadequate image resolution.

The problem of segmentation of kidney MR images has not been extensively studied. In [1], a region growing segmentation algorithm is proposed to identify the regions of medulla and cortex. This algorithm uses a global threshold to form regions with similar connecting regions, thus resulting in separation of the medulla and cortex. Although this method has proved to be successful, it has some limitations. Firstly, setting of a global threshold does not take into account the local intensity variations. Secondly, it does not account for the intensity inhomogeneity and the heterogeneity present in the cortex region.

Another technique, first makes use of principal component analysis (PCA) to eliminate temporal redundancy and noise, then in the next step, k-means clustering of principal components (PCs) is performed to identify the regions of medulla and cortex [2]. Despite the success of this method in dynamic contrast enhanced (DCE)-MR images of the kidney, it has some drawbacks. For instance, it fails to identify the cortex correctly, as the k-means clustering divides the cortex into two regions which is not desirable. This observation can be attributed to the heterogeneity of the cortex and medulla, i.e. intensities of the cortex and medulla mix into each other. Moreover, k-means clustering suffers from several limitations, including a high degree of sensitivity to initialization of the cluster centers, sensitivity to outliers and skewed distributions, and a tendency to converge to a local minimum [3]. Some other techniques to segment renal compartments in the human kidney using DCE-MR kidney images are presented in [4]. These techniques rely on the perfusion of the contrast agent into the tissue. Studies that are not based on DCE cannot rely upon this method.

Some work has also been done in segmenting the whole kidney from abdominal MR scans. These methods have been described in [5-7]. These methods, respectively, use level set method, graph cuts and connectivity, and neural networks to segment a whole kidney from abdominal MR images.

Since the kidney MR images exhibit intensity variations between the different tissue classes, thresholding techniques can be used. To this end, histogram thresholding, which is the most popular intensity-based thresholding technique, could be used. However, it fails at the object boundaries due to blurring and uncertainty in deciding pixel intensities. To compensate this limitation, intuitionistic fuzzy sets (IFS) are used. The IFS represent the vagueness associated with the pixel intensities via non-membership and hesitancy values in addition to a membership function. Although IFS thresholding scheme was originally proposed to segment color images, this method is now being used to segment brain MR images [8]. In addition to this, IFS have also been used to segment other medical images as in [9], [10].

In this paper, we propose a novel method using IFS to segment the kidney MR images. To our knowledge, it is the first application which uses IFS representation and thresholding scheme for segmenting kidney MR images. The main contributions of this paper are three-fold: defining a novel membership function to create intuitionistic fuzzy representation of the image; using the Hamming distance to compute histon; and using a multi-level thresholding scheme to segment kidney MR images.

The proposed novel membership function creates an intuitionistic fuzzy representation of the image which compensates for the inherent heterogeneity within the tissue class and the overall intensity inhomogeneity present in the kidney MR images. The proposed method also partitions the kidney MR image into four regions: medulla, cortex, blood vessels, and pelvis. The rest of the paper is organized as follows: Section II gives a brief description of intuitionistic fuzzy sets. Section III describes the proposed algorithm. Section IV presents the experimental results and quantitative evaluation, while section V presents concluding remarks from the authors.

II. INTUITIONISTIC FUZZY SET

Fuzzy set theory was proposed by Zadeh [11], where each element is allowed to belong or not belong to a finite set at the same time, i.e. a degree of membership or belongingness is assigned to each element, which implies that the degree of non-membership is 1 minus the degree of membership. However, in many cases, this simple representation is inadequate to represent data. Hence, Attanassov introduced the concept of intuitionistic fuzzy sets (IFS) which is now popularly known as A-IFS [12], [13]. The concept of A-IFS states that the degree of non-membership is not simply equal to 1 minus the degree of membership, but there might be some uncertainty in deciding the degree of non-membership. This uncertainty can be quantified by defining a third parameter, known as the degree of hesitation or intuitionistic fuzzy (IF) index.

Consider a finite fuzzy set A defined on a universe of discourse $X = \{x_1, x_2, ..., x_n\}$. An IFS [12-13] in X can be represented mathematically as:

$$A = \{x, \mu_A(x), \nu_A(x), \pi_A(x) | x \in X\} \qquad (1)$$

such that $\mu_A(x)$, $\nu_A(x)$, $\pi_A(x) : X \to [0,1]$ denote the functions for the degree of membership, degree of non-membership and degree of hesitancy respectively of an element x in the finite set X. It is to be noted that $\mu_A(x)$ and $\nu_A(x)$ should satisfy the mandatory condition $0 \le \mu_A(x) + \nu_A(x) \le 1$. Consequently, it is necessary that $\mu_A(x) + \nu_A(x) + \pi_A(x) = 1$.

III. PROPOSED ALGORITHM

A. Proposed Membership function

In this paper, a novel membership function is formulated by using the restricted equivalence function (REF), which is one of the many types of membership function. Let f_1 and f_2 be two automorphisms in a unit interval, then $REF(x, y)$ is mathematically given as [14]:

$$REF(x, y) = f_1^{-1}(1 - |f_2(x) - f_2(y)|) \qquad (2)$$

with $c(x) = f_2^{-1}(1 - f_2(x))$, "$c$" is a strong negation such that $c : [0,1] \to [0,1]$ that adheres to the conditions mentioned in [14]. Restricted equivalence function is defined as follows. A function REF: $[0,1]^2 \to [0,1]$ is said to be a restricted equivalence function if it satisfies all the necessary conditions [14].

T. Chaira used the restricted equivalence membership function to perform single level thresholding to segment blood vessels from its background [15]. However, in this paper, a modified restricted equivalence function is proposed to take into account the heterogeneity present between the different tissue classes of the kidney.

Let $f_2(x) = x$, hence according to the definition of restricted equivalence function in (2) now becomes, $REF(x, y) = f_1^{-1}(1 - |x - y|)$.

Now let $f_1(x) = \ln[x(e-1)+1]$, where $e = \exp(1)$ [15]. Therefore, the restricted equivalence function now becomes:

$$REF(x, y) = (e^{1 - |x - y|} - 1) / (e - 1) \qquad (3)$$

Simplifying, eq. (3) becomes $REF(x, y) = 0.582(e^{1 - |x - y|} - 1)$, where $1/(e-1) = 0.582$. This REF is defined as the membership function membership function since its range is $[0,1]$. Hence it is renamed as:

$$\mu(x) = REF = 0.582(e^{1 - |x - y|} - 1) \qquad (4)$$

where x and y relate to image pixel intensity and mean for a certain threshold "t" [15]. Given that segmentation of kidney MR images is a multi-level thresholding problem, equation (4) would generate multiple membership functions which complicates the computation. Moreover, subtraction of the mean of local intensities from the current pixel intensity will perform a homogenization operation which will nullify the intensity variations between the different tissue classes of the kidney MR image. Hence, to avoid the aforesaid scenario, the mean of the object region is not considered, i.e. y=0, which modifies equation (4) as:

$$\mu(x) = 0.582(e^{1 - x} - 1) \qquad (5)$$

The above function also satisfies all the necessary conditions of restricted equivalence functions mentioned in [14].

B. A-IFS Representation of image

Intuitionistic fuzzy (IF) representation of an image has been used previously in [15] and [16] for segmenting medical images. A-IFS representation of an image is constructed using an intuitionistic fuzzy generator (IFG). Consider an image of size $M \times N$, having intensity levels in the range of 0 to L-1. The IFS representation of the image is given as:

$$I = \{(x_{ij}, \mu_I(x_{ij}), \nu_I(x_{ij}), \pi_I(x_{ij})\} \qquad (6)$$
$$\text{for } i = 1, 2, 3, ..., M, j = 1, 2, 3, ..., N$$

where $\mu_I(x_{ij}), \nu_I(x_{ij})$ and $\pi_I(x_{ij})$ represent the degree of membership, non-membership and hesitancy respectively of each pixel at the $(i, j)^{th}$ location.

The degree of membership $\mu_I(x_{ij})$ for each pixel x_{ij} in image I is computed using equation (5). In an image composed of several regions, the variations in the pixel intensities are more noticeable near the boundaries between two objects, and on the contrary are more or less constant inside the object region. This implies that the hesitancy in deciding the pixel intensities will be more at the object boundaries and less inside the object region. Therefore, the degree of hesitancy $\pi_I(x_{ij})$ at each location will be proportional to the absolute difference of the membership degree and the mean of the membership degree at that location [17].

$$\pi_I(x_{ij}) = (1 - \mu_I(x_{ij})) \frac{\left| \mu_I(x_{ij}) - \mu_I^a(x_{ij}) \right|}{\max\left(\max\left(\left| \mu_I(x_{ij}) - \mu_I^a(x_{ij}) \right|\right)\right)} \qquad (7)$$

The average intensity $\mu_I^a(x_{ij})$ can be calculated as $\mu_I^a(x_{ij}) = \sum_{k=-1}^{1} \sum_{l=-1}^{1} \mu_I(g_{(i+k)(j+l)}) h(i+k, j+l)$, where h is the filter mask, for $i = 1, 2, 3, ... M$ and $j = 1, 2, ..., N$. In equation (7), multiplication by $(1 - \mu_I(x_{ij}))$ ensures that $\pi_I(x_{ij})$ is always constrained between 0 and 1. It also ensures that the constraint $0 \le \mu_I(x_{ij}) + \nu_I(x_{ij}) \le 1$ is always satisfied. The degree of non-membership for every pixel is hence given by $\nu_I(x_{ij}) = 1 - \mu_I(x_{ij}) - \pi_I(x_{ij})$.

C. Computation of A-IFS Histon

The histon was introduced as a contour plotted over the existing histogram [18], with the purpose of eliminating the ambiguity and uncertainty present at the object boundaries. The primary function of the histon is to group the pixels of similar intensity values under one intensity level. The similarity is decided by various similarity or divergence measures, and the belongingness of a pixel intensity value to a particular group intensity is decided by a Gaussian membership function.

The IF histon at the gth intensity level, represented by $F(g)$, is mathematically expressed as:

$$F(g) = \sum_{m=1}^{M} \sum_{n=1}^{N} (1 + \mu(m,n)) \delta(I(m,n) - g), 0 \le g \le L - 1$$
$$(8)$$

where $\mu(m,n)$ is the Gaussian function given as:
$\mu(m,n) = \exp\left(-\frac{1}{2}\left(\frac{d_T(m,n)}{\sigma}\right)^2\right)$, where σ is the standard deviation of the similarity matrix d_T (see eq. 9). The choice of

a Gaussian membership function is motivated by the smooth transition exhibited between the degree of membership and non-membership [8].

In this paper, we propose to use Hamming distance as a similarity measure to select the pixels with similar intensity values. Consider a $P \times Q$ neighborhood around a pixel $I(m,n)$, then the cumulative distance of all the pixels in the pixel neighborhood is given by:

$$d_T(m,n) = \sum_{p \in P} \sum_{q \in Q} d_H(I(m,n), I(p,q)) \qquad (9)$$

where $d_H(I(m,n), I(p,q))$ is the Hamming distance between two pixels $I(m,n)$ and $I(p,q)$, which is given as [19]:

$$d_H(I(m,n), I(p,q)) = \left| \mu_I(m,n) - \mu_I(p,q) \right| + \left| \nu_I(m,n) - \nu_I(p,q) \right| + \left| \pi_I(m,n) - \pi_I(p,q) \right| \qquad (10)$$

D. Intuitionistic Fuzzy Roughness Measure

The rough set theory, introduced by Pawlak [20], proposes to model every vague or imprecise concept by mapping it into an approximation space. The approximation space is represented by a pair of exact concepts, which are known as the upper approximation and the lower approximation. Since IFS histon at a particular intensity level accounts for all the pixels with similar intensity values, therefore, it can be regarded as an upper approximation. On the contrary, histogram can be associated with the lower approximation as histogram value at a particular intensity represents all the pixels with that intensity. Hence, the IF roughness measure $r(g)$ can be defined as [17]:

$$r(g) = 1 - \frac{f(g)}{F(g)}, \text{ for } 0 \le g \le L - 1 \qquad (11)$$

where $f(g)$ denotes the histogram value at the gth intensity level.

The peaks and valleys in histogram of an image, respectively, represent different regions and the boundaries between these regions. But, this representation is inaccurate due to the uncertainty in pixel intensities caused by blurring at the object boundaries. In such cases, the IF roughness measure provides an accurate representation of different regions of an image. The peaks in IF roughness measure represent uniform regions, but not all peaks stand for significant regions in an image. Therefore, significant peaks are chosen by enforcing a criterion that the minimum distance between two peaks should be 35. The value for the minimum peak distance is chosen empirically. Consequently, optimum thresholds levels are determined to segment the kidney MR images.

Fig. 1(a) and Fig. 1(b), respectively show histogram and histon plots. It can be noted that due to noise and heterogeneity in image, valley points are not represented precisely in Fig. 1(a). However, IF roughness measure given in Fig. 1(b) provides a better representation of peaks and valleys which can be used to segment kidney MR images.
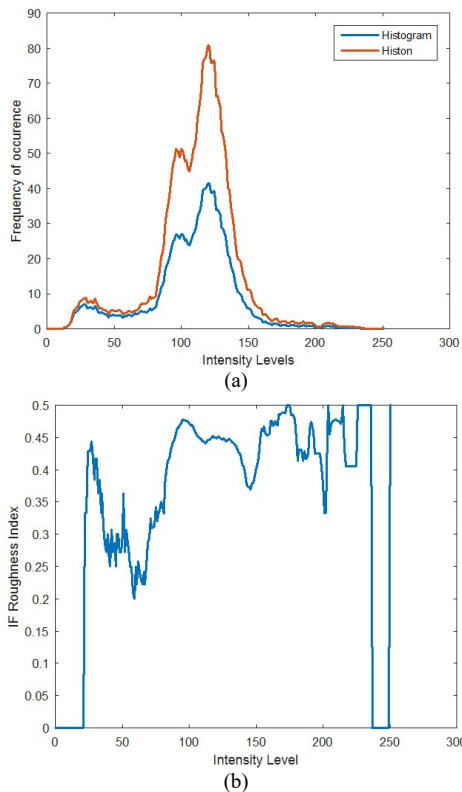
Fig. 1. (a) Histogram and Histon for the kidney MR image (slice 5 of time point 1). (b) Intuitionistic Fuzzy Roughness Measure for the kidney MR image.
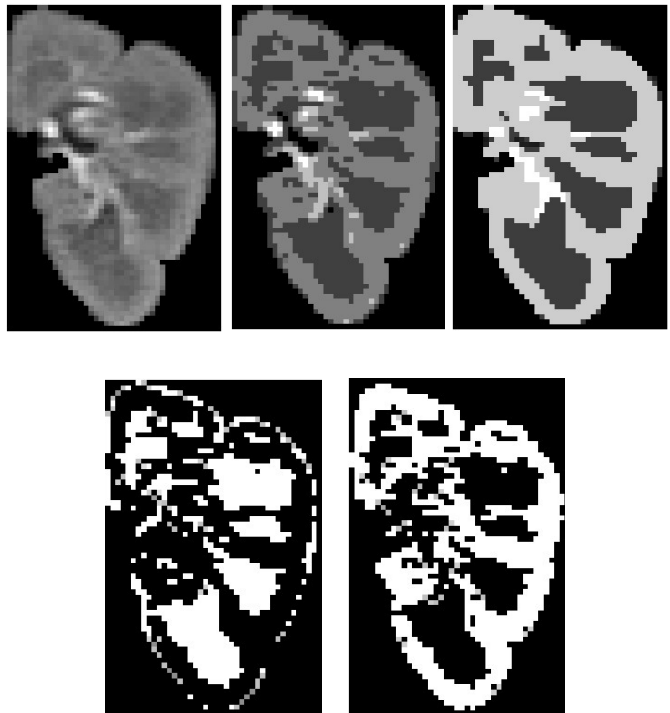

Fig. 2. The results of segmentation using the proposed algorithm. The top row has original Image, segmented image, ground truth (left to right). Bottom row has the region of medulla and region of cortex (left to right).

IV. EXPERIMENTAL RESULTS

The proposed method is applied on kidney MR images acquired at the Center for NMR Research, Pennsylvania State University College of Medicine, Hershey, PA. A breath-held, multi-echo gradient echo scan was utilized to collect T2* weighted data on a single volunteer. The relaxation time (TR) was 30 ms and 6 echo times were acquired (4.95, 8.61, 12, 16.7, 21, 26.5 ms), of which only the first echo time was used. The image volume was a coronal 3D slab of size $224 \times 182 \times 16 \times 4$. The manual segmentation (ground truth) for these images were obtained with the help of a radiologist. For quantitative analysis, a 2D coronal slice (slice no. 5) at each time point was chosen.

A. Qualitative Analysis

The result of segmentation using the proposed method on the kidney MR images is depicted in Fig. 2 such that the top row shows the original image, segmented image and ground truth in the order as shown (column-wise). The bottom row shows the region of medulla and the region of cortex respectively (column-wise). By observing Fig. 2, it can be concluded that the segmentation results are consistent with the ground truth.

B. Quantitative Evaluation

The qualitative analysis of the results of segmentation is highly subjective, and hence can vary from person-to-person. Hence, quantitative analysis of the results of segmentation is performed so as to provide a platform for comparison with the results of different methods.

TABLE I. CONFUSION TABLE WITH FALSE POSITIVES AND FALSE NEGATIVES FOR MEDULLA AND CORTEX USING THE PROPOSED ALGORITHM.

Time Point	Classified Pixels	Ground Truth		
		Medulla	Cortex	FP
1	Medulla	97.13	1.67	1.67
	Cortex	1.69	97.32	1.69
	FN	1.69	1.67	
2	Medulla	95.37	3.17	3.17
	Cortex	1.98	94.67	1.98
	FN	1.98	3.17	
3	Medulla	98.56	2.14	2.14
	Cortex	1.76	98.39	1.76
	FN	1.76	2.14	
4	Medulla	94.45	4.68	4.68
	Cortex	4.01	95.21	4.01
	FN	4.01	4.68	

The accuracy of segmentation can be determined by a confusion table [21], which has segmented tissue classes as the rows, and tissue classes in ground truth as columns. A confusion table reports the percentage of false positives (FP), false negatives (FN), true negatives (TN) and true positives (TP. True positive (TP) for each class is the diagonal entry of the table. True negative (TN) of a class is the percentage of pixels that are not members of this particular class. False negative (FN) of each class represents the percentage of the class in ground truth which was mistakenly classified into other classes. False Positive (FP) of each class is given by the percentage of the pixels which were incorrectly classified into a class over the pixels that do not belong to the class in ground truth.

TABLE I depicts the confusion table of results of the proposed segmentation algorithm. The medulla and cortex tissue

classes are the only significant renal components in disease diagnosis [1]. Therefore, the confusion matrix is shown only for these tissue classes. The ground truth is indicated in the top row of the confusion table while the left column shows the classified results. The value in each cell is calculated as the percentage with respect to ground truth. For example, 97.13% pixels of true medulla are classified as class medulla. 1.67% pixels are incorrectly classified into class medulla. False negative (FN) of 1.69% for medulla implies these pixels are of medulla class in ground truth but not classified as medulla. A false positive (FP) of 1.67% for class medulla means these pixels are misclassified as medulla.

Three more performance parameters to evaluate the performance of the proposed segmentation algorithm can be computed based upon true positives (TP), false positives (FP), true negatives (TN) and false negatives (FN). These performance parameters are given as [22]:

1. Percentage of negative false segmentation, i.e. under segmentation $UnS = FP/TN$.

2. Percentage of positive false segmentation, i.e. over segmentation $OvS = FN/TP$.

3. Percentage of overall false segmentation, i.e. incorrect segmentation $InS = (FP+FN)/N$.

Here N denotes total number of pixels in that class. TABLE II shows these three performance parameters expressed as % for kidney MR images. It can be observed that under segmentation and incorrect segmentation is very low (less than 2%) which highlights the accuracy of the proposed algorithm. Fig. 3 shows performance parameters calculated in TABLE II.

The performance of the proposed segmentation can also be evaluated by computing the Dice coefficient [23]. The Dice coefficient is the ratio of relative overlap between the segmentation results and the ground truth, and is mathematically defined as:

$$DC(S_1, S_2) = \frac{2|S_1 \cap S_2|}{|S_1| + |S_2|} \qquad (12)$$

S_1 and S_2 represent the numbers of pixels classified into a particular class using the proposed restricted equivalence membership intuitionistic fuzzy segmentation (REMIFS) method and the ground truth, where $|.|$ denotes the cardinality of a set. The Dice coefficients (DC) of the REMIFS method are compared with those of the k-means clustering (KMC) method. TABLE III indicates that the DC value for both medulla and cortex is higher than KMC method. It can be noted that the DC value for cortex using REMIFS method is significantly higher than using the KMC method, which is consistent with the limitation of KMC algorithm.

V. CONCLUSION

This paper presents an intuitionistic fuzzy theory based thresholding algorithm for the segmentation of kidney MR

images. A novel membership function is proposed to deal with the pixel intensity variations and heterogeneity present in the

TABLE II. THREE PERFORMANCE PARAMETERS- UNDER SEGMENTATION (UNS), OVER SEGMENTATION (OVS) AND INCORRECT SEGMENTATION (INS) EXPRESSED AS % FOR SEGMENTED KIDNEY MR IMAGES.

Time Point	Tissue Class	Performance parameter in %		
		UnS	OvS	InS
1	Medulla	1.71	1.73	0.53
	Cortex	1.73	1.71	0.32
2	Medulla	3.34	2.07	0.8
	Cortex	2.07	3.34	0.49
3	Medulla	2.17	1.78	0.61
	Cortex	1.78	2.17	0.37
4	Medulla	4.91	4.24	1.36
	Cortex	4.24	4.91	0.82
Average	Medulla	3.03	2.45	0.82
	Cortex	2.45	3.03	0.5

TABLE III. COMPARISON OF DICE COEFFICIENTS FOR KIDNEY MR IMAGES SEGMENTED USING THE PROPOSED REMIFS AND KMC [2] METHODS.

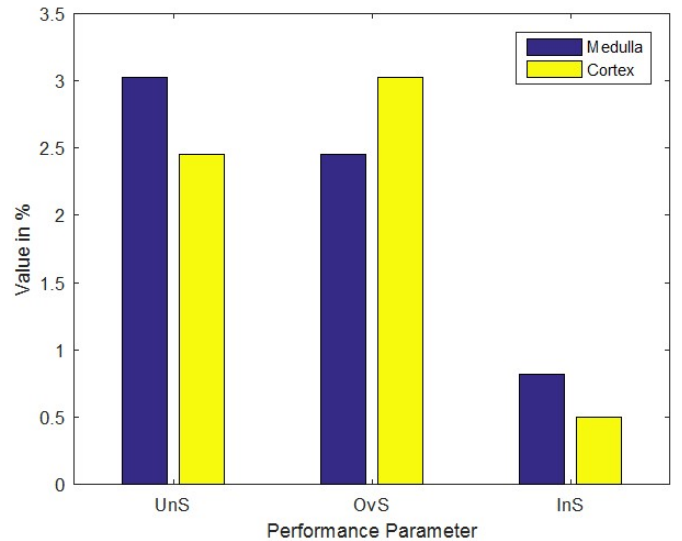| Time Point	Tissue Class	Dice Coefficient	
		KMC	REMIFS
1	Medulla	0.947	0.956
	Cortex	0.923	0.958
2	Medulla	0.914	0.920
	Cortex	0.938	0.941
3	Medulla	0.905	0.908
	Cortex	0.939	0.935
4	Medulla	0.937	0.953
	Cortex	0.927	0.948

Fig. 3. Bar graph representation of the performance parameters of the segmentation results. Values of under segmentation (UnS), over segmentation (OvS), and incorrect segmentation (InS) obtained for medulla and cortex for the kidney MR image in Fig. 2(a).

tissue classes of the kidney MR images. The kidney tissue is segmented into medulla, cortex, and blood vessels, of which only medulla and cortex classes are used for performance

evaluation due to their clinical significance. The performance of REMIFS was compared with the existing k-means clustering algorithm using the Dice coefficient. The results of the comparison demonstrate improved performance of the REMIFS algorithm relative to KMC. Despite its advantage over the existing technique, the performance of REMIFS algorithm can be further improved. For instance, the REMIFS algorithm can be integrated with the k-means clustering to further enhance its performance. These possibilities will be investigated in future work.

REFERENCES

[1] D. Lv *et al*., "Dynamic Contrast-Enhanced Magnetic Resonance Images of the Kidney," in *IEEE Engineering in Medicine and Biology Magazine*, vol. 27, no. 5, pp. 36-41, September-October 2008.

[2] X. Yang, H. Le Minh, T. Cheng, K. H. Sung, W. Liu, "Automatic Segmentation of Renal Compartments in DCE-MRI Images," *Medical Image Computing and Computer Assisted Intervention*, Springer Link, vol. 9349, pp. 3-11.

[3] S. N. Sulaiman and N. A. Mat Isa, "Adaptive fuzzy-K-means clustering algorithm for image segmentation," in *IEEE Transactions on Consumer Electronics*, vol. 56, no. 4, pp. 2661-2668, November 2010.

[4] F. G. Zollner, S. Li, J. Roervik, A. Lundervold, L. Schad, "Segmentation of renal compartments in DCE-MRI of human kidney", *In Proc. 7th Int. Symp. on Image and Signal Proc.* (ISPA), pp. 744-748, Sept. 4-6, 2011, Dubronvik Croatia..

[5] M. Shehata *et al*., "A level set-based framework for 3D kidney segmentation from diffusion MR images," *Image Processing (ICIP), 2015 IEEE International Conference on*, Quebec City, QC, 2015, pp. 4441-4445.

[6] A. K. Rudra et.al, "Kidney segmentation using graph cuts and pixel connectivity," Pattern Recognition Letters, vol. 34, pp. 1470-1475, 2013.

[7] N. Goceri and E. Goceri, "A Neural network based kidney segmentation for MR images," 14th IEEE Int. Conf. Machine Learning and Applications (ICMLA), pp. 1195-1198, Miami, FL, 2011.

[8] Y. K. Dubey and M. M. Mushrif, "Intuitionistic fuzzy roughness measure for segmentation of brain MR images," Advances in Pattern Recognition (ICAPR), 2015 Eighth International Conference on, Kolkata, pp. 1-6, 2015.

[9] Y. K. Dubey and M.M. Mushrif, "Segmentation of brain MR images using intuitionistic fuzzy clustering algorithm," in ICVGIP, IIT Bombay. ACM, 2012, 978-1-4503-1660-6/12/12.

[10] M.R. Mookiah *et.al*, "Automated detection of optic disk in retinal fundus images using intuitionistic fuzzy histon segmentation." Journal of Engineering in Medicine, vol. 227, no. 1, pp. 37-49, January 2013.

[11] L.A. Zadeh, "Concept of a linguistic variable and its application to approximate I, II, III," *Inf. Sci.*, vol. 8, pp. 199-249, 301-357, 43-80, 1985.

[12] K.T. Attanassov, *Intuitionistic Fuzzy Sets, Theory, and Applications* (Series in Fuzziness and Soft Computing). Heidelberg, Germany: Physica-Verlag, 1999.

[13] K.T. Attanassov, "Intuitionistic Fuzz Set," *Fuzzy Sets Syst.*, vol. 20, pp. 87-97, 1986.

[14] H. Bustince, E. Barrenechea, and M. Pagola, "Restricted equivalence function," *Fuzzy Sets Syst.*, vol. 157, no. 17, pp. 2333-2346, 2006.

[15] T. Chaira, "Intuitionistic Fuzzy Segmentation of Medical Images," in *IEEE Transactions on Biomedical Engineering*, vol. 57, no. 6, pp. 1430-1436, June 2010.

[16] A. Jati, *et.al*, "A novel segmentation approach for noisy medical images using intuitionistic fuzzy divergence with neighborhood-based membership function," Journal of Microscopy, vol. 257, issue 3, pp. 187-200, 2015.

[17] M. M. Mushrif and A. K. Ray, "A-IFS Histon Based Multithresholding Algorithm for Color Image Segmentation," in *IEEE Signal Processing Letters*, vol. 16, no. 3, pp. 168-171, March 2009.

[18] A. Mohabey and A.K. Ray, "Fusion of rough set theoretic approximations and FCM for color image segmentation," in IEEE *Int. Conf. Systems, Man, and Cybernetics*, 2000, pp. 1529-1534.

[19] I. Montes, N. R. Pal, V. Janiš and S. Montes, "Divergence Measures for Intuitionistic Fuzzy Sets," in *IEEE Transactions on Fuzzy Systems*, vol. 23, no. 2, pp. 444-456, April 2015.

[20] Z. Pawlak, "Rough set theory and its applications," International Journal of Computer Information Sciences, vol. 11, pp. 341-356, 1982.

[21] H. Wang and B. Fei, "A modified fuzzy c-means classification method using a multiscale diffusion filtering scheme," Medical Image Analysis, vol. 13, pp. 193-202, 2009.

[22] Shan Shen, W. Sandham, M. Granat and A. Sterr, "MRI fuzzy segmentation of brain tissue using neighborhood attraction with neural-network optimization," in *IEEE Transactions on Information Technology in Biomedicine*, vol. 9, no. 3, pp. 459-467, Sept. 2005.

[23] U. Vovk, F. Pernus, and B. Likar, "A review of methods for correction of intensity inhomogeneity in MRI," IEEE Transaction on Medical Imaging, vol. 26, no. 3, pp. 405-415, March 2007.